Polyvinylidene fluoride coated optical fibre for detecting perfluorinated chemicals

Polyvinylidene Fluoride Coated Optical Fibre for Detecting Perfluorinated Chemicals

Fairuza Faiz[a], Gregory Baxter[b], Stephen Collins[b], Fotios Sidiroglou[b], Marlene Cran[a,*]

[a]Institute for Sustainable Industries and Liveable Cities, Victoria University, PO Box 14428, Melbourne, Vic 8001, Australia

[b]Telecommunications, Electronics, Photonics and Sensors Research Group, Victoria University, PO Box 14428, Melbourne, Vic 8001, Australia

*Corresponding author: marlene.cran@vu.edu.au

Abstract: This work reports the development of a Fabry-Perot Interferometry (FPI) based optical fibre to detect perfluorooctanoic acid (PFOA) and other perfluoroalkyl substances (PFAS) in aqueous solutions. A novel and simple sensor fabrication procedure utilizing an immersion precipitation-based phase inversion process to form a thin polyvinylidene fluoride (PVDF) coating at the end-faces of freshly cleaved optical fibres is presented. The PVDF coating was rich in the electroactive β-phase, which enhances dipole-dipole and hydrophobic interaction with PFAS at binding sites. Sensor testing with model PFOA solutions showed that the PVDF coated FPI optical fibre can detect PFOA. The change in optical path difference (OPD) with change in PFOA concentration was considered as a measure of sensitivity and it corresponded to a value of 0.9 to 5 nm/ppm for PFOA. In real PFAS solutions obtained from fire-fighting foams, this value was found to be significantly more sensitive at 178 nm/ppb.

Keywords: perfluorooctanoic acid; perfluoroalkyl substances; optical fiber sensors; Fabry-Perot interferometry; polyvinylidene fluoride

1 Introduction

Contamination of water and land by perfluoroalkyl substances (PFAS) has been reported in many parts of the world in recent years [1, 2]. The discovery of organic fluorochemicals in human serum and the environment has initiated growing interest in characterising the effects and the extent of their presence in the environment [3-5]. Perfluorooctane sulfonate (PFOS), perfluorooctanoic acid (PFOA), perfluorohexane sulfonate, and perfluorononanoic acid are among the common forms of PFAS which have been studied extensively [6, 7]. They are commonly found in surfactants, aerosol propellants, insecticide, refrigerants, anaesthetics, and plastics [8] and are used in the production of non-stick cookware, food packaging, fire-fighting foams, and some water and oil proof fabrics [9, 10]. Recent reports show that locations of PFAS contaminated land, ground water or reservoir are usually close to manufacturing plants [11], or

near military bases [12], airports and firefighters' training grounds [13]. Many of these have a history of using a specific fire retardant, namely aqueous film-forming foam (AFFF) [13, 14]. The fluorinated components present in AFFF, typically PFOA and PFOS, are dispersed during military or fire training exercises or during actual fire extinguishing events and are suspected to be the cause of the environmental pollution.

Due to the inherent strength of the C-F bond, PFAS do not readily biodegrade and are known to accumulate once released into the environment [15] which can present a health risk to humans and animals who may consume PFAS contaminated food or water. It has been reported that PFAS may adversely affect foetal growth and learning behaviour in children, decrease fertility, increase cholesterol, cause hormone dysfunction, affect the immune system, and increase the risk of cancer [15]. Several studies on a population exposed to very high levels of PFOA have suggested that it strongly correlates to various diseases including kidney and testicular cancer, ulcerative colitis, thyroid disease, hypertension and high cholesterol [16]. Both PFOA and PFOS are listed in the Stockholm Convention on Persistent Organic Pollutants, which prohibits their production and the import or export of foams containing either or both chemicals in more than 180 countries [17].

Environment Protection Agencies or equivalents around the globe have expressed the need to monitor these contaminants, while addressing issues regarding regulation and development of adaptive frameworks like the National Environment Management Plan (NEMP) [18] to respond to emerging research and knowledge. Based on scientific reports and evidence, Food Standards Australia New Zealand (FSANZ) has considered 0.56 to 5 ppb of PFOA and 0.07 ppb of PFOS in drinking water to be the maximum safe level for human consumption [19]. The tolerable daily intake values for PFAS, including PFOS and PFOA, recommended by FSANZ is 160 nanograms per kilogram of body weight per day [20].

Current detection methods for PFOA and PFOS contaminants in water are based on conventional techniques such as liquid chromatography coupled with mass spectrometry (MS) or tandem MS [21, 22] or gas chromatography coupled with MS [23]. These are all costly and time-consuming processes that often require complicated pre-treatment steps, expensive labour resources, and are inapplicable for *in situ* measurements and analysis [7]. Molecularly imprinted polymer-based portable sensors have been proposed to address this issue, but they are unable to differentiate between different types of PFAS and require long fabrication times [24-26]. A smartphone-based system developed recently as a portable PFAS detector is

susceptible to variation in weather conditions [24]. In addition, there is a lack of information regarding the effect of temperature on sensitivity of these portable sensors, their cross-sensitivity to other contaminants, and in some cases the generation of toxic wastes. There is a clear need for robust, portable sensing systems that can be used in the field and fibre optic sensors may be suitable for this application due to their many inherent advantages. Optical fibre sensors (OFS) are known for their small size, immunity to electromagnetic interference, passiveness and intrinsic safety, high sensitivity and bandwidth, multiplexing capability, chemical inertness, and robustness to hostile environments. Additionally, sensors based on optical fibres are suitable for remote sensing operations and are compatible with online continuous monitoring applications. As the technology is portable [27], it can be easily configured to provide real time information on any physical, chemical or biological measurand in a field test. More importantly, chemical sensing functionality of OFS can be further enhanced by coating chemically selective optical materials at the end-face of optical fibres as in Fabry–Perot interferometric (FPI) fibre optic sensors. A comparison between the conventional methods of PFAS analysis and/or detection and FPI based OFS is provided in Table 1.

Table 1 Summary of current PFAS analysis and detection methods.

Technique	Advantages	Disadvantages	References
GC-MS LC-MS	▪ High accuracy ▪ Good selectivity and reliability ▪ Limit of detection is in ppt range	▪ Time consuming preparation steps ▪ Requires bulky instruments ▪ Requires trained personnel ▪ Non-portable ▪ Complex data analysis technique ▪ Expensive	[28-32]
Smart-phone colorimetric analysis	▪ Portability, field application ▪ Rapid analysis ▪ Readily available kit	▪ Not selective to PFAS, can detect other surfactants ▪ Low detection limit ▪ Toxic chemicals needed ▪ Toxic waste generated	[24]
FPI based OFS	▪ Portability, field application ▪ Convenient and economic ▪ Can be used for remote sensing and real time continuous monitoring options ▪ Easily optimized ▪ Light weight	▪ Susceptible to temperature variation ▪ Stabilizes slowly in aqueous solution ▪ Functionalization procedures are time consuming ▪ Sensitivity is subject to functionalization ▪ Limit of detection is in ppm range	[33-35]

Fabry–Perot interferometric fibre optic sensors have been demonstrated for monitoring humidity [36, 37], acoustic wave intensity [38], magnetic fields [39], mechanical vibrations [40], marine phosphate [41] and temperature [42, 43]. Most of these FPI sensors are analogous to an optically transparent material with two mirror-like surfaces, whereby the distance or refractive index between the surfaces can vary to bring about changes in path difference of reflected light beams. Generally, FPI sensor fabrication techniques reported in literature include processes such as chemical or physical vapour deposition [44, 45], laser micromachining [46], ionic self-assembly monolayer process (ISAM) [47], splicing [48] and dip coating [49]. Among these fabrication methods, etching or laser micromachining involve hazardous and complex protocol, whereas others, such as the ones that form the FPI sensors from two separate fibres bonded through the use of an external casing [50] or splicing [42], cause excessive coupling loss or low reflectivity issues in the end product.

The ability to detect contaminants in water using FPI relies on the affinity of the contaminant for the coating on the end of the fibre to induce a signal. Polyvinylidene fluoride (PVDF) is a hydrophobic polymer that has widespread usage in water treatment facilities and can be easily functionalized and processed to form thin films using phase inversion [51-53]. Utilizing a PVDF coating on the sensor can utilize the polymer's ferroelectric properties due to the presence of the beta (β) or gamma (γ) phase in the polymer structure. The surface charge on PVDF can help in binding with PFOA in aqueous solution through dipole-dipole or hydrophobic interactions, since the contaminant has a carboxylate group that interacts strongly with polar substances and also an octyl group, which is inert and hydrophobic. A recent study has provided further evidence that PVDF is compatible for use with optical fibre sensors, that offers numerous advantages over conventional electrical or electrochemical sensors including portability, remote sensing and real time monitoring in underground wells and bore holes [33].

In this work, we report the development and testing of a PVDF coated FPI fibre optic sensor for detecting PFAS in aqueous solutions. The PVDF coating, developed using a phase inversion process based on a freshly cleaved end-face of a standard telecommunication grade single mode optical fibre, was tested in model PFOA solutions followed by real AFFF solutions. The potential for sensitivity to temperature variations was also performed. To the best of our knowledge, this is the first report of PFAS detection by PVDF coated optical fibre. Moreover, there are no other reports of forming a PVDF coating at the end-face of an optical fibre using the method described herein.

2 Materials and Methods

2.1 Materials

The PVDF polymer used was Solef 1015 obtained as a powder from Solvay (Australia). Solvents *N*,*N*-dimethylformamide (DMF), polyvinyl butyral (butvar) and chloroform were obtained from Sigma-Aldrich (Australia). The PFOA with a purity of 95% was also purchased from Sigma-Aldrich (Australia). A sample of AFFF was obtained as a diluted solution and was analysed by an external laboratory for its composition (see Table S1 in Supplementary Material). Ultrapure (Milli Q) water was used throughout the experiments and no chemical reagent was modified prior to its usage.

2.2 Optical Spectrum Analyzer Setup

The experimental setup incorporating the optical fibre sensor for determining the PFOA concentration consisted of an ANDO AQ6317B Optical Spectrum Analyzer (OSA), an Erbium Broadband Source (EBS) from MPB Communications Inc. and a three-port optical circulator as shown in the schematic Figure 1. It also included a ThermoScientific table-top incubator for maintaining a constant environmental temperature surrounding the sensor probe. Temperature readings were acquired using a K-type thermocouple connected to a Fluke 52 II electronic thermometer.

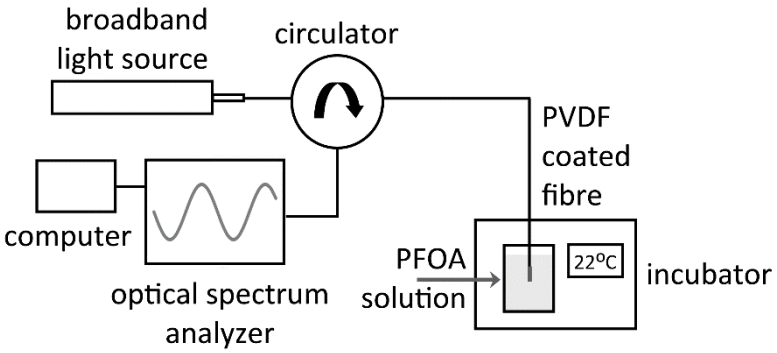

Figure 1. Schematic of the experimental setup

For data acquisition purposes, the OSA resolution was set at 0.1 nm and the centre wavelength at 1565 nm with a span of 11 nm. The sampling rate was set at 1001 points over the 1520-1610 nm wavelength range. Automated continuous data acquisition was achieved through a GPIB card and LabVIEW interface, while further data analysis of the recorded spectral information was performed using MATLAB and Microsoft Excel. A photograph of the actual apparatus is presented in the Supplementary Material (Figure S1).

2.3 Optical Fibre Coating

The PVDF coating solution was formed by heating 1.67 g of PVDF powder in 14 mL of DMF at 80 °C for 1 h under constant stirring. To promote good adhesion between the optical fibre glass and PVDF, 0.03 g of the cross-linking agent Butvar was first dissolved in 2 mL of chloroform and then added to the homogenous PVDF solution mixture at 80 °C and mixed thoroughly with a stirrer to avoid agglomeration. The solution was allowed to cool to room temperature. Stripped, cleaned and cleaved optical fibres were manually dipped vertically into the PVDF solution for 5-10 s and to a depth of 1-2 cm at room temperature and were then immersed vertically into a beaker containing ultrapure water for 10-20 s to induce coagulation and develop the coating. To obtain a satisfactory thickness of the thin film on the fibre end-face, the dipping procedure was repeated while allowing enough time for a coated layer to dry in between subsequent intervals. Similar PVDF films were obtained by dip coating glass slides in the solution for characterization. A flow diagram of the dipping procedure is presented in the Supplementary Material (Figure S2).

2.4 Coating Characterization

A Perkin-Elmer Frontier Fourier-transform infrared (FTIR) spectrophotometer with a diamond attenuated total reflectance (ATR) crystal was used for characterization of the PVDF coating and identifying its phase composition. Film samples were cast on glass slides in accordance with the method described in section 2.3, were peeled from the slide then clamped onto the ATR crystal. A minimum of 32 scans were performed over the wavenumber range 4000-650 cm^{-1} with a minimum of 5 samples averaged. A Hitachi TM3030 Plus Tabletop SEM using an accelerating voltage of 15 kV in backscattering mode was used for obtaining images of the PVDF coatings on optical fibre end faces. Samples were coated with iridium prior to obtaining the images.

2.5 Quantification of PFOA Adsorption

A sample of 1 mg/L PFOA solution was prepared and a section of PVDF film was soaked for several hours. Samples of the PFOA solution before and after soaking in PVDF were sent to ALS Water (Scoresby Victoria) where they were subjected to quantitative analysis in accordance with NATA accredited ALS Method EP231X.

2.6 Sensor Selection

The raw spectral data obtained from a PVDF coated optical fibre, using the experimental set up shown in Figure 1, were normalized against the reflection spectrum of a cleaved fibre end-face taken before splicing the sensor to the system. A normalized spectrum, free of source modulation effects that showed a sinusoidal curve was considered an indication of a good sensor from the perspective of data analysis. Only coated fibres that displayed such characteristics in their normalized spectra were selected for further experimentation.

2.7 Measurement of Temperature Response

The experimental setup shown in Figure 1 was used to determine the sensitivity of the PVDF coated fibre to variations in temperature in water. The incubator thermostat setting was changed to vary the temperature of water in which the PVDF coated fibre was submerged and maintained until the temperature of the water stabilized to that value and data acquisition was completed. The PVDF coated fibre was first stabilized at a temperature close to the room temperature for several hours and then subjected to the actual temperature variation test. The temperature was then increased or decreased in steps of 10 °C between 22 to 60 °C and measurements at specific intervals were taken when the coated fibre had stabilized and the temperature reading on the thermometer was steady.

2.8 Measurement of Response to PFOA

A 100 ppm PFOA stock solution was prepared by dissolving 0.01 g of PFOA in 100 mL of ultrapure water under heating at 80 °C for 10 minutes. Test solutions of concentrations ranging between 10 to 60 ppm were obtained by diluting the stock solution. The PVDF coated fibre was stabilized in 20 mL of ultrapure water at a temperature of 23.8 °C and data acquisition was performed using the setup shown in Figure 1. After stabilization, a known volume of the PFOA stock solution was added to the submerged PVDF coated fibre to form a desired concentration and data acquisition was performed following stabilization in the PFOA solution. The addition of PFOA, stabilization and data acquisition were repeated until all the spectral information at different concentrations of PFOA were obtained.

2.9 Measurement of Response to AFFF Solution

A sample of diluted AFFF with known concentrations of PFAS was used in this test. The solution was comprised of different PFAS compounds as shown in the Supplementary Material (Table S1) and was confirmed to contain a total of 1.14 ppb of total PFAS. The steps used to

measure the response to different concentrations of the AFFF were the same as those presented in section 2.8.

3 Results and Discussion

3.1 Sensor Description and Operating Principle

Figure 2 shows a schematic of the low finesse PVDF coated fibre formed by dip coating and immersion precipitation. The PVDF coating acts as a Fabry-Perot (FP) etalon that reflects light from the two interfaces as shown in Figure 2. The reflected light waves interfere to produce a resultant reflection spectrum, which is sensitive to changes in the PVDF coating's physical thickness, refractive index or both. A change in PFOA or PFAS concentration brings about a change in the thickness of the PVDF coating due to molecular interaction and attachment of the analyte to the surface of the thin film. This in turn causes a phase difference between the reflected beams from the inner and outer surface of the FP etalon by altering the optical path difference (OPD) between them and leads to the resultant interferogram being shifted. In the experiments, the wavelength shift in the spectrum was monitored in real time using the OSA and the variation in OPD with analyte concentration change was measured after data acquisition to determine sensor performance.

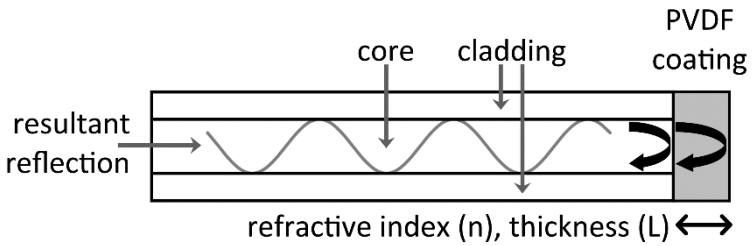

Figure 2. Schematic of PVDF coated optical fibre

Equation (1), represents an expression of the overall reflected light intensity from the FPI sensor for a two-beam interference model. This was used to simulate the normalized reflection spectra and curve fitting to determine OPD from the coefficient of fitted curves.

$$I = I_1 + I_2 + 2\gamma\sqrt{I_1 I_2}\ cos\left(\frac{4\pi nL}{\lambda} + \phi_0\right) \quad (1)$$

Here, I_1 and I_2 and are the intensities of the reflected rays from the PVDF coating's inner and outer boundaries, γ is the degree of coherence, ϕ_0 is the initial phase difference of the reflected intensities, λ is the wavelength of light in free-space, and n and L are the refractive index and

thickness of the PVDF thin film respectively. The product of *n* and *L* is the OPD which was determined by curve fitting techniques and used as a measure of sensitivity in this work.

Mathematical modelling with equation (1) has shown that varying the initial thin film thickness (L) affects the number of peaks and troughs present in an interferogram as well as their positions on an intensity versus wavelength graph. This can have implications from a data acquisition or analysis point of view, which alludes to the fact that an interferogram with the necessary combination of peaks/troughs generated for monitoring should be within the available spectral window formed by the combination of the EDFA broadband source and optical spectrum analyzer used in the experimental arrangement for this work.

3.2 Characterization of PVDF Coating and PFOA Adsorption

The FTIR spectra of a typical PVDF film depicts characteristic peaks at 840 and 1275 cm^{-1} [54] which are representative of the electroactive β-phase of PVDF (see Figure S3 in the Supplementary Material). This supports the presence of surface charge on the PVDF coating which has been considered to play an important role in selectively attracting the PFOA molecules in solution to the binding sites on the coating. Analysis of PFOA concentrations before and after PVDF film immersion confirmed that *ca*. 10% of PFOA was adsorbed on to the PVDF film. Furthermore, the SEM images shown in Figure 3(a) and (b) show differences in the surface morphology of PVDF films before and after exposure to PFOA. The presence of nodule like structures on the surface in Figure 3(b) may be an indication of the clusters/micelles of PFOA reported previously [55] that may have formed due to the hydrophobic or dipole-dipole interaction of PFOA molecules with PVDF.

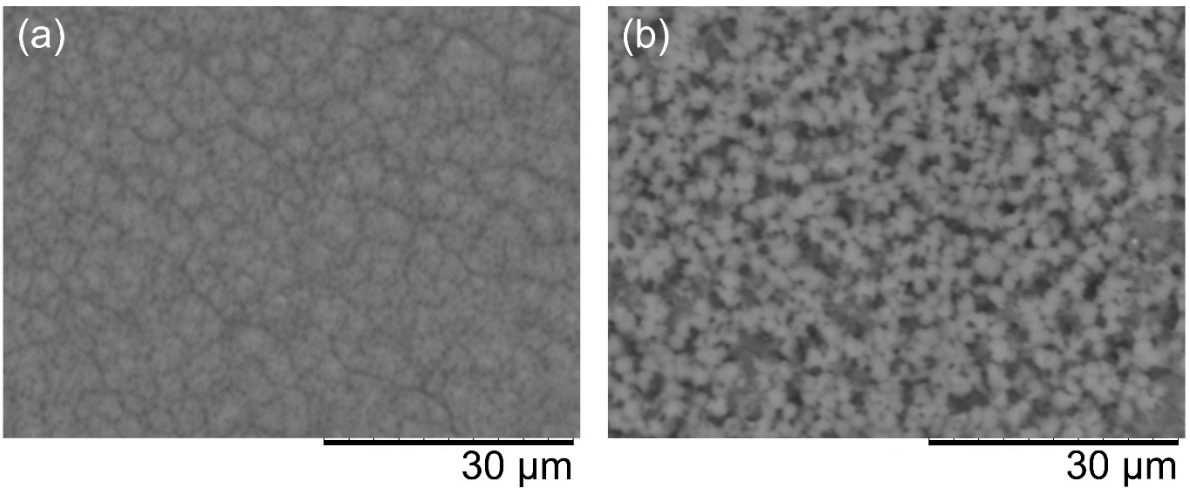

Figure 3. SEM images of PVDF film surface: (a) before and (b) after immersion in PFOA

3.3 Response of Sensor to Temperature Variation

The reflection spectra exhibit a redshift or peak wavelength (λ_p) shift towards the higher wavelength region, as shown in Figure 4 (a), with increasing temperature in water. This implies that the changes in OPD are primarily the result of changes in physical thickness due to thermal expansion. There is an added effect of a changed refractive index of the surrounding medium, which creates an impact on the wavelength shift and cause the final spectrum to be different from that in air. The spectral wavelength shift is therefore dependent on the optical thickness which is linked to the characteristics of the ambient medium in the immediate vicinity of the sensor.

Both the peak wavelength shift and OPD shown in Figure 4 (a) and (b) exhibit a linear response over the test temperature range of 20-60 °C with a resulting temperature sensitivity of 3.9 nm/°C calculated as change in OPD per unit change in temperature. This suggests that, outside of the controlled laboratory set up, the OPD change with temperature variation must be compensated in order to correctly determine the PVDF coated fibre's response to PFOA or other analytes. The issue of temperature cross sensitivity for field sensing applications can be addressed by using a rare earth doped fluorescence intensity ratio based optical fibre temperature sensors [56-58] in conjunction with the PVDF coated fibre. Fluorescence intensity ratio based temperature sensing has been shown to be one of the most successful in the past demonstrating a sensitivity in the order of 1.1 to 1.6% change in the measurand per degree Celsius, which is much higher than that of the FBG (7×10^{-4} %/°C) [59].Thus, to eliminate the effect of temperature sensitivity from the PFOA detection test in the present study, experiments with the PVDF coated fibre were performed under constant temperature conditions. The subsequent protocol adopted for performing the sensitivity test of the PVDF coated fibre to the PFOA/PFAS concentrations therefore assumed that the OPD change observed is only due to the change in analyte concentration and not as a result of temperature variation.

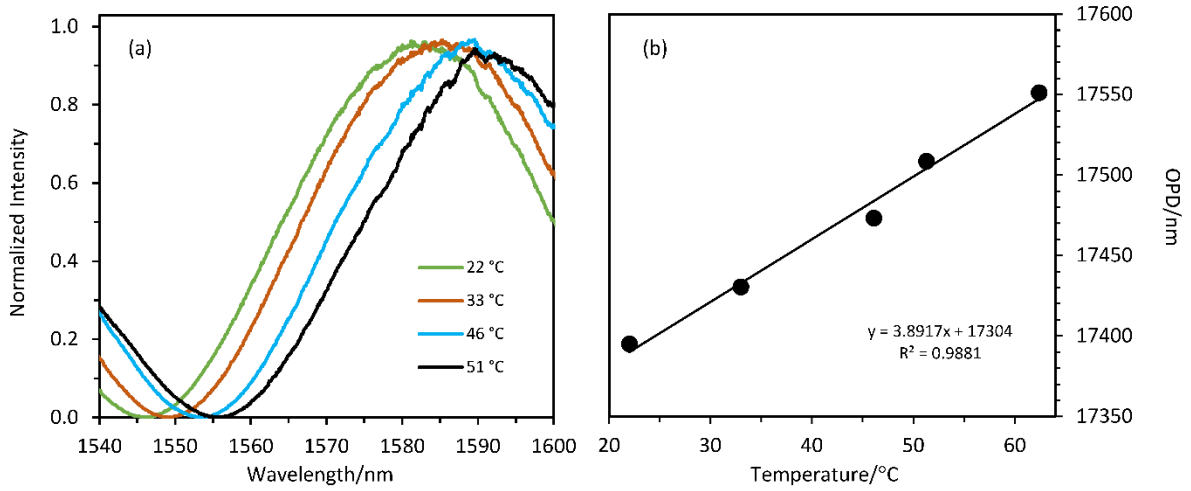

Figure 4. Effect of temperature change on: (a) peak wavelength shift in FPI spectra and (b) variation in OPD (color version available online)

3.4 Response of Sensor to PFOA

The raw sensor spectra obtained for in PFOA solution of different concentrations at a constant temperature of 23.8 °C is shown in Figure 5 (a). The method of PFOA detection based on FPI involved observation of wavelength shifts using the setup shown in Figure 1 and the measurement of OPD from individual fitted spectral data was determined using Excel. Curve fit parameters generated by the mathematical model given by equation (1) resulted in values of n and L at specific concentration. Correlation between the normalized spectral response from the coated fibre and the Excel fits (Figure 5 (b)) were found to be in the order of 0.96~0.99.

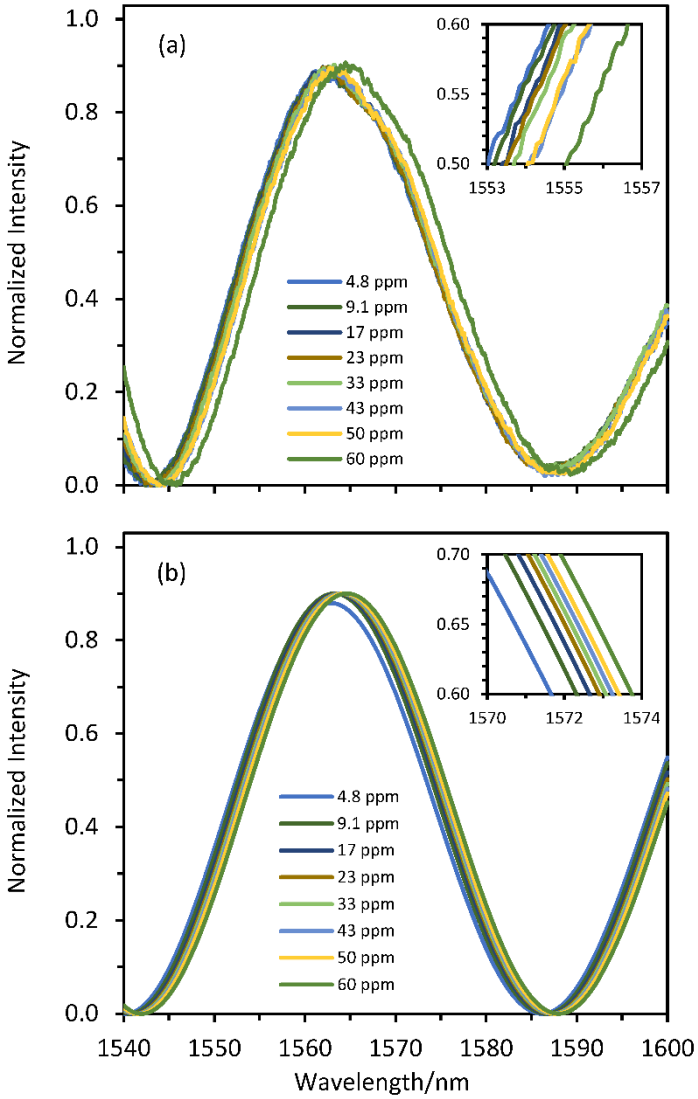

Figure 5. Sensor response to change in PFOA concentration: (a) raw data, and (b) fitted curves (b) where zoomed inlays show increasing concentration left to right from 0 to 60 ppm (color version available online)

Calculations were performed on the actual normalized spectra using equation (2):

$$\left(\frac{4\pi nL}{\lambda_1} + \phi_0\right) - \left(\frac{4\pi nL}{\lambda_2} + \phi_0\right) = 2\pi \qquad (2)$$

where λ_1 and λ_1 are the wavelengths of the adjacent peaks or troughs. In this case, the expected value of L was 18333 to 18380 nm over the PFOA concentration range 4.8 and 60 ppm when the value of n was 1.42.

The SEM image of the cross section of a PVDF coated fibre has revealed a coating thickness ranging between 10-40 μm on the optical fibre (see Figure S4 in the Supplementary Material). Excel fits rendered the L values 18710 and 18732 nm over the chosen range which falls within this limit (i.e. 18.7 μm) and the average values was then used for the OPD analysis shown in Figure 6.

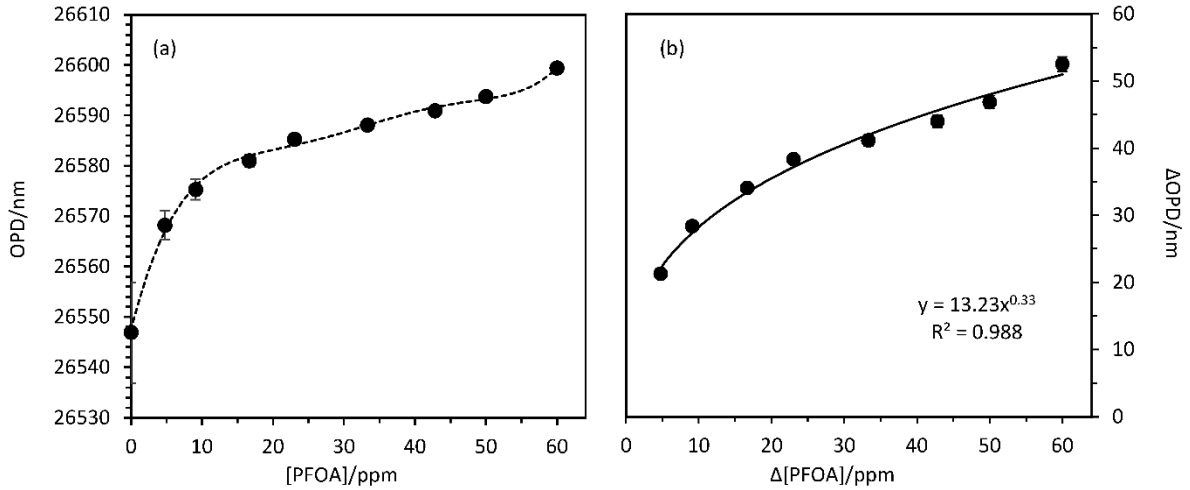

Figure 6. Effect of PFOA concentration on: (a) OPD, and (b) change in OPD with fitted equation

From the analysis of the OPD plots shown in Figure 6 (a), it was assumed that PFOA adsorption on the surface of the PVDF membrane increases with increasing concentration of PFOA until all the binding sites are occupied and the film surface is saturated. The development of a layer of PFOA is therefore assumed to cause a change in the apparent thickness of the PVDF coating on the end of the fibre which results in a change in the OPD value. The sensitivity of the coated fibre was derived from the OPD plot and is nonlinear as shown in Figure 6 (b) with the fit obtained given by equation (3):

$$\Delta OPD = 13.23 \times \Delta[PFOA]^{0.33} \quad (3)$$

It was observed that the sensor's sensitivity (i.e. ΔOPD /Δ[PFOA]) varies from approximately 5 nm/ppm to 0.9 nm/ppm over the tested concentration range. The small errors associated with the measurements (see Figure 6), also suggest s reasonably high level of accuracy within the measurements. Furthermore, through separate careful experimental procedures carried out using a range of low PFOA concentrations between 0.1 ppb and 1 ppb, it was observed that the PVDF coated fibre did not produce significant wavelength shift when the PFOA concentration

was below 5 ppm (see Figure S5 in supplementary material). The limit of detection for PFOA concentration was therefore considered to be approximately 5 ppm.

3.5 Response of Sensor to AFFF

The PVDF coated fibre has shown a positive response to the model compound PFOA but at relatively high concentrations. In real samples, the composition of PFAS is more diverse with a range of different compounds at different concentrations. The spectral data obtained for the measurement of the PVDF coated fibre response to AFFF is presented in Figure 7(a), where a sensitivity in the ppb range was obtained. This observation has important implications for further development of the coated fibre as a potential field sensor where real contaminated water sources will have similar compositions to the sample of AFFF solution used in this study. Although the results do not confirm whether the response is derived from a specific compound in the AFFF mixture, it may be used as a screening test to show the presence of general PFAS compounds. From the OPD plot versus concentration in Figure 7(b) the linear fit of the data points suggest a sensitivity of 178 nm/ppb (i.e. OPD change per ppb) of PFAS, which is considerably higher than the PFOA sensitivity mentioned above and sensitivity of other reported sensors [35] within this range of concentrations. Moreover, the low errors associated with the data as depicted by the error bars in Figure 7(b) are an indication of a high level of accuracy associated with the measurements. The response to other PFAS in the ppb range may suggest that the actual limit of detection could be lower and it may be dependent on parameters like surface morphology, availability of binding sites etc., which varied in the case of each individual sensor. It may also suggest that the PVDF is more sensitive to PFOS since the concentration was nearly thirty times higher than PFOA in the AFFF. Further evaluation of the selectivity is therefore required in order to assess the suitability of the PVDF coated fibre to detect these emerging contaminants. The addition of zeolites or other active sites to the PVDF, for example, may enhance the selectivity towards particular AFFF components thereby improving the suitability of the sensor for robust field applications.

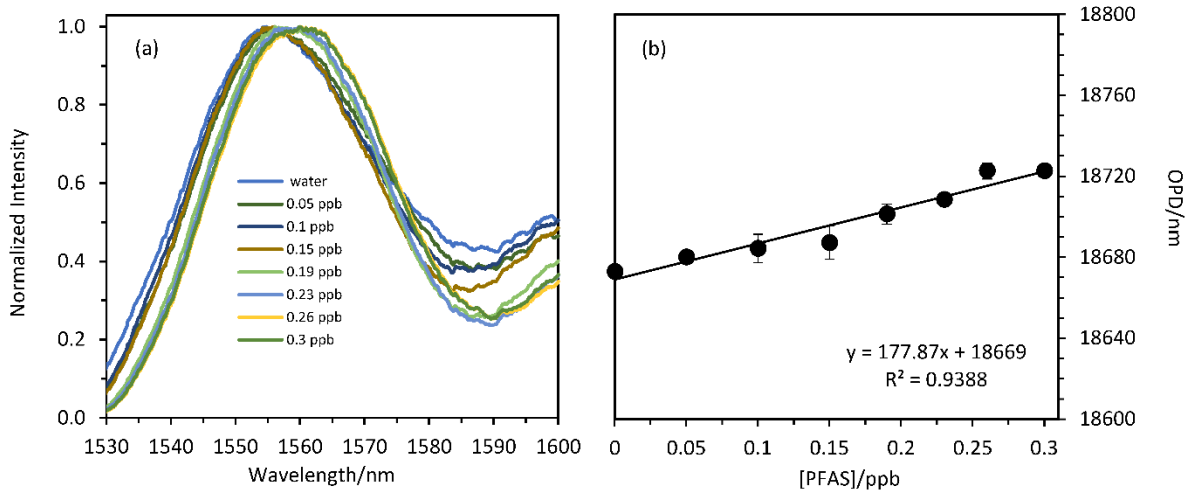

Figure 7. Effect of AFFF concentration on: (a) spectral shift and (b) change in OPD where zoomed inlay in (a) shows increasing concentration left to right from 0 to 0.3 ppb (color version available online)

4 Conclusions

In this study, a novel optical fibre coating system using PVDF was developed, optimized and tested in order to measure the concentration of PFAS in aqueous solutions. The system, based on the principle of FPI, was shown to be sensitive to temperature variations although this can be compensated or corrected accordingly. The PVDF film was shown to effectively adsorb PFOA from model aqueous solutions. Testing of the sensors in the PFOA solutions showed a detection sensitivity of 0.9 to 5 nm/ppm. Further testing in real AFFF solutions showed improved sensitivity of 178 nm/ppb. This work has demonstrated a concept for the future development of a feasible FPI sensor utilizing a PVDF coating for the field detection of PFAS in the natural environment.

5 Acknowledgements

This work was supported by Victoria University International Postgraduate Research Scholarship.

6 Competing Interests Declaration

The authors declare no conflict of interest.

7 References

[1] EPA Victoria, Land and Groundwater, PFAS in Victoria, https://ref.epa.vic.gov.au/your-environment/land-and-groundwater/pfas-in-victoria, 2019, (accessed 12 August 2019).

[2] C. Kunacheva, S. Fujii, S. Tanaka, S. Seneviratne, N.P.H. Lien, M. Nozoe, et al., Worldwide surveys of perfluorooctane sulfonate (PFOS) and perfluorooctanoic acid (PFOA) in water environment in recent years, Water Sci Technol, 66(2012) 2764-71, https://doi.org/10.2166/wst.2012.518.

[3] C.A. Moody, W.C. Kwan, J.W. Martin, D.C. Muir, S.A. Mabury, Determination of perfluorinated surfactants in surface water samples by two independent analytical techniques: liquid chromatography/tandem mass spectrometry and ^{19}F NMR, Anal Chem, 73(2001) 2200-6, https://doi.org/10.1021/ac0100648.

[4] C.A. Moody, J.A. Field, Perfluorinated surfactants and the environmental implications of their use in fire-fighting foams, Environ Sci Technol, 34(2000) 3864-70, https://doi.org/10.1021/es991359u.

[5] K.J. Hansen, H.O. Johnson, J.S. Eldridge, J.L. Butenhoff, L.A. Dick, Quantitative characterization of trace levels of PFOS and PFOA in the Tennessee River, Environ Sci Technol, 36(2002) 1681-5, https://doi.org/10.1021/es010780r.

[6] T. Tran.T, J. Li, H. Feng, J. Cai, L. Yuan, N. Wang, et al., Molecularly imprinted polymer modified TiO2 nanotube arrays for photoelectrochemical determination of perfluorooctane sulfonate (PFOS), Sens Actuators B Chem, 190(2014) 745-51, http://dx.doi.org/10.1016/j.snb.2013.09.048.

[7] J. Gong, T. Fang, D. Peng, A. Li, L. Zhang, A highly sensitive photoelectrochemical detection of perfluorooctanic acid with molecularly imprined polymer-functionalized nanoarchitectured hybrid of AgI–BiOI composite, Biosens Bioelectron, 73(2015) 256-63, https://doi.org/10.1016/j.bios.2015.06.008.

[8] J. Liang, X. Deng, K. Tan, An eosin Y-based "turn-on" fluorescent sensor for detection of perfluorooctane sulfonate, Spectrochim Acta A Mol Biomol Spectrosc, 150(2015) 772-7, https://doi.org/10.1016/j.saa.2015.05.069.

[9] Australian Health Protection Principal Committee, Per- and poly-fluoroalkyl substances (PFAS) FactSheet https://www.health.gov.au/internet/main/publishing.nsf/Content/A12B57E41EC9F326CA257BF0001F9E7D/$File/PFAS-factsheet-15June2016.pdf, 2016, (accessed 3 October 2019).

[10] C.J. McMurdo, D.A. Ellis, E. Webster, J. Butler, R.D. Christensen, L.K. Reid, Aerosol enrichment of the surfactant PFO and mediation of the water−air transport of gaseous PFOA, Environ Sci Technol, 42(2008) 3969-74, https://doi.org/10.1021/es7032026.

[11] X.C. Hu, D.Q. Andrews, A.B. Lindstrom, T.A. Bruton, L.A. Schaider, P. Grandjean, et al., Detection of Poly- and Perfluoroalkyl Substances (PFASs) in U.S. Drinking Water Linked to Industrial Sites, Military Fire Training Areas, and Wastewater Treatment Plants, Environ Sci Technol Lett, 3(2016) 344-50, https://doi.org/10.1021/acs.estlett.6b00260.

[12] ABC Radio Adelaide, PFAS chemicals probe expanded around Adelaide's Edinburgh airbase, https://www.abc.net.au/news/2018-05-17/edinburgh-adelaide-raaf-pfas-contamination-fears/9770162?pfmredir=sm, 2018, (accessed 30 August 2019).

[13] R. Turner, Firefighting foam contamination: DFES confirms chemicals found in bore near training site, ABC News, https://www.abc.net.au/news/2016-10-14/dfes-toxic-chemical-contamination-confirmed/7934334, 2016, (accessed 10 September 2019).
[14] S. Lerner, The U.S. military is spending millions to replace toxic firefighting foam with toxic firefighting foam, The Intercept, https://theintercept.com/2018/02/10/firefighting-foam-afff-pfos-pfoa-epa/, 2018, (accessed 10 September 2019).
[15] ATSDR, Health Effects of PFAS, https://www.atsdr.cdc.gov/pfc/health_effects_pfcs.html, 2016, (accessed 10 March 2019).
[16] W. Nicole, PFOA and cancer in a highly exposed community: new findings from the C8 science panel, Environ Health Perspect, 121(2013) A340, https://dx.doi.org/10.1289%2Fehp.121-A340.
[17] C. Hogue, Governments endorse global PFOA ban, with some exemptions, Chemical and Engineering News, https://cen.acs.org/environment/persistent-pollutants/Governments-endorse-global-PFOA-ban/97/web/2019/05, 2019, (accessed 10 September 2019).
[18] EPA Victoria, PFAS National Environmental Management Plan, https://www.epa.vic.gov.au/for-community/environmental-information/land-groundwater-pollution/pfas-national-environmental-management-plan, 2019, (accessed 1 December 2019).
[19] Australian Government Department of Health, Health Based Guidance Values for Per- and Poly-Fluoroalkyl Substances (PFAS), https://www1.health.gov.au/internet/main/publishing.nsf/Content/ohp-pfas-hbgv.htm, 2019, (accessed 1 December 2019).
[20] CRC Care, PFAS practitioner guide, https://www.crccare.com/knowledge-sharing/pfos-and-pfoa-guidelines, 2019, (accessed 12 March 2018).
[21] K. Risha, J. Flaherty, R. Wille, W. Buck, F. Morandi, T. Isemura, Method for trace level analysis of C8, C9, C10, C11, and C13 perfluorocarbon carboxylic acids in water, Anal Chem, 77(2005) 1503-8, https://doi.org/10.1021/ac0490548.
[22] W.M. Young, P. South, T.H. Begley, G.O. Noonan, Determination of Perfluorochemicals in Fish and Shellfish Using Liquid Chromatography–Tandem Mass Spectrometry, J Agric Food Chem, 61(2013) 11166-72, https://doi.org/10.1021/jf403935g.
[23] C.A. Huset, A.C. Chiaia, D.F. Barofsky, N. Jonkers, H.-P.E. Kohler, C. Ort, et al., Occurrence and mass flows of fluorochemicals in the Glatt Valley watershed, Switzerland, Environ Sci Technol, 42(2008) 6369-77, https://doi.org/10.1021/es703062f.
[24] C. Fang, X. Zhang, Z. Dong, L. Wang, M. Megharaj, R. Naidu, Smartphone app-based/portable sensor for the detection of fluoro-surfactant PFOA, Chemosphere, 191(2018) 381-8, https://doi.org/10.1016/j.chemosphere.2017.10.057.
[25] N. Cennamo, L. Zeni, G. D'Agostino, G. Porto, A. Biasiolo, Optical chemical fiber sensor for the detection of perfluorinated compounds in water, IEEE International Instrumentation and Measurement Technology Conference (I2MTC), (2018) 1-5 pp, https://doi.org/10.1109/I2MTC.2018.8409736.

[26] N. Cennamo, L. Zeni, P. Tortora, M.E. Regonesi, A. Giusti, M. Staiano, et al., A High Sensitivity Biosensor to detect the presence of perfluorinated compounds in environment, Talanta, 178(2018) 955-61, https://doi.org/10.1016/j.talanta.2017.10.034.

[27] T. Liu, W. Wang, D. Jian, J. Li, H. Ding, D. Yi, et al., Quantitative remote and on-site Hg^{2+} detection using the handheld smartphone based optical fiber fluorescence sensor (SOFFS), Sens Actuators B Chem, 301(2019) 127168, https://doi.org/10.1016/j.snb.2019.127168.

[28] J.T. Watson, O.D. Sparkman, Introduction to Mass Spectrometry: Instrumentation, Applications, and Strategies for Data Interpretation: John Wiley & Sons; 2007.

[29] A. El Aneed, A. Cohen, J. Banoub, Mass spectrometry, review of the basics: electrospray, MALDI, and commonly used mass analyzers, Appl Spectrosc Rev, 44(2009) 210-30, https://doi.org/10.1080/05704920902717872.

[30] X. Zhao, J. Li, Y. Shi, Y. Cai, S. Mou, G. Jiang, Determination of perfluorinated compounds in wastewater and river water samples by mixed hemimicelle-based solid-phase extraction before liquid chromatography–electrospray tandem mass spectrometry detection, J Chromatogr A, 1154(2007) 52-9, https://doi.org/10.1016/j.chroma.2007.03.093.

[31] D.J. Torres, To Run or to Fly: A Comparison Between HPLC and GC, https://bitesizebio.com/29109/run-fly-comparison-hplc-gc/, 2019, (accessed

[32] M. Trojanowicz, M. Koc, Recent developments in methods for analysis of perfluorinated persistent pollutants, Microchim Acta, 180(2013) 957-71, 10.1007/s00604-013-1046-z.

[33] X. Li, M. Yang, J. Dai, H. Liu, D. Yin, L. Dong, Optical fiber humidity sensor with PVDF thin film as sensitive element, paper 78533T, Proc. SPIE 7853, Advanced Sensor Systems and Applications IV, 9 November, 2010, https://doi.org/10.1117/12.871725.

[34] B.E. Jones, Optical fibre sensors and systems for industry, Journal of Physics E: Scientific Instruments, 18(1985) 770-82, http://dx.doi.org/10.1088/0022-3735/18/9/007.

[35] N. Cennamo, G. D'Agostino, G. Porto, A. Biasiolo, C. Perri, F. Arcadio, et al., A Molecularly Imprinted Polymer on a Plasmonic Plastic Optical Fiber to detect perfluorinated compounds in water, Sensors, 18(2018) 1836, https://doi.org/10.3390/s18061836.

[36] L.H. Chen, T. Li, C.C. Chan, R. Menon, P. Balamurali, M. Shaillender, et al., Chitosan based fiber-optic Fabry–Perot humidity sensor, Sens Actuators B Chem, 169(2012) 167-72, https://doi.org/10.1016/j.snb.2012.04.052.

[37] J.S. Santos, I.M. Raimundo Jr, C.M. Cordeiro, C.R. Biazoli, C.A. Gouveia, P.A. Jorge, Characterisation of a Nafion film by optical fibre Fabry–Perot interferometry for humidity sensing, Sens Actuators B Chem, 196(2014) 99-105, https://doi.org/10.1016/j.snb.2014.01.101.

[38] L.H. Chen, C.C. Chan, W. Yuan, S.K. Goh, J. Sun, High performance chitosan diaphragm-based fiber-optic acoustic sensor, Sens Actuators A Phys, 163(2010) 42-7, https://doi.org/10.1016/j.sna.2010.06.023.

[39] K.D. Oh, J. Ranade, V. Arya, A. Wang, R.O. Claus, Optical fiber Fabry-Perot interferometric sensor for magnetic field measurement, IEEE Phot Technol Lett, 9(1997) 797-9, https://doi.org/10.1109/68.584994.

[40] T.K. Gangopadhyay, Prospects for fibre Bragg gratings and Fabry-Perot interferometers in fibre-optic vibration sensing, Sens Actuators A Phys, 113(2004) 20-38, https://doi.org/10.1016/j.sna.2004.01.043.

[41] J.M. Zhu, Y. Shi, X.Q. Zhu, Y. Yang, F.H. Jiang, C.J. Sun, et al., Optofluidic marine phosphate detection with enhanced absorption using a Fabry–Pérot resonator, Lab on a Chip, 17(2017) 4025-30, https://doi.org/10.1039/C7LC01016H.

[42] H.Y. Choi, K.S. Park, S.J. Park, U.-C. Paek, B.H. Lee, E.S. Choi, Miniature fiber-optic high temperature sensor based on a hybrid structured Fabry–Perot interferometer, Opt Lett, 33(2008) 2455-7, https://doi.org/10.1364/OL.33.002455.

[43] L. Li, Z. Feng, X. Qiao, H. Yang, R. Wang, D. Su, et al., Ultrahigh sensitive temperature sensor based on Fabry–Pérot interference assisted by a graphene diaphragm, IEEE Sens J, 15(2015) 505-9, https://doi.org/10.1109/JSEN.2014.2361174.

[44] C. Lin, A.J. Steckl, J. Scofield, SiC thin-film Fabry-Perot interferometer for fiber-optic temperature sensor, IEEE Trans Elect Dev, 50(2003) 2159-64, https://doi.org/10.1109/TED.2003.816106.

[45] P. Hajireza, K. Krause, M. Brett, R. Zemp, Glancing angle deposited nanostructured film Fabry-Perot etalons for optical detection of ultrasound, Opt Expr, 21(2013) 6391-400, https://doi.org/10.1364/OE.21.006391.

[46] E. Cibula, D. Đonlagić, Miniature fiber-optic pressure sensor with a polymer diaphragm, Appl Opt, 44(2005) 2736-44, https://doi.org/10.1364/AO.44.002736.

[47] F.J. Arregui, Y. Liu, I.R. Matias, R.O. Claus, Optical fiber humidity sensor using a nano Fabry–Perot cavity formed by the ionic self-assembly method, Sens Actuators B Chem, 59(1999) 54-9, https://doi.org/10.1016/S0925-4005(99)00232-4.

[48] T. Zhu, T. Ke, Y. Rao, K.S. Chiang, Fabry–Perot optical fiber tip sensor for high temperature measurement, Opt Commun, 283(2010) 3683-5, https://doi.org/10.1016/j.optcom.2010.05.037.

[49] J. Liu, Y. Sun, X. Fan, Highly versatile fiber-based optical Fabry-Pérot gas sensor, Opt Expr, 17(2009) 2731-8, https://doi.org/10.1364/OE.17.002731.

[50] B. Yu, G. Pickrell, A. Wang, Thermally tunable extrinsic Fabry-Perot filter, IEEE Phot Technol Lett, 16(2004) 2296-8, https://doi.org/10.1364/FIO.2004.FWH23.

[51] D.-J. Lin, C.-L. Chang, T.-C. Chen, L.-P. Cheng, Microporous PVDF membrane formation by immersion precipitation from water/TEP/PVDF system, Desalination, 145(2002) 25-9, https://doi.org/10.1016/S0011-9164(02)00340-5.

[52] G. Mago, D.M. Kalyon, F.T. Fisher, Membranes of polyvinylidene fluoride and PVDF nanocomposites with carbon nanotubes via immersion precipitation, J Nanomater, 2008(2008) 17, http://dx.doi.org/10.1155/2008/759825.

[53] H. Shi, F. Liu, L. Xue, Fabrication and characterization of antibacterial PVDF hollow fibre membrane by doping Ag-loaded zeolites, J Membr Sci, 437(2013) 205-15, https://doi.org/10.1016/j.memsci.2013.03.009.

[54] X. Cai, T. Lei, D. Sun, L. Lin, A critical analysis of the α, β and γ phases in poly (vinylidene fluoride) using FTIR, RSC Adv, 7(2017) 15382-9, https://doi.org/10.1039/C7RA01267E.

[55] N. Lundquist, M.J. Sweetman, K. Scroggie, M. Worthington, L. Esdaile, S. Alboaiji, et al., Polymer supported carbon for safe and effective remediation of PFOA-and PFOS-contaminated water, ACS Sustainable Chem Eng, 7(2019) 11044-9, https://doi.org/10.1021/acssuschemeng.9b01793.

[56] S.A. Wade, S.F. Collins, K.T.V. Grattan, G.W. Baxter, Strain-Independent Temperature Measurement by Use of A Fluorescence Intensity Ratio Technique in Optical Fiber, Appl Opt, 39(2000) 3050-2, https://doi.org/10.1364/AO.39.003050.

[57] G.W. Baxter, S.A. Wade, S.F. Collins, G. Monnom, E. Maurice, Rare-Earth-Doped Optical Fibers for Point Temperature Sensing, Doped Fiber Devices, International Society for Optics and Photonics1996, pp. 249-56.

[58] F. Sidiroglou, S.A. Wade, N.M. Dragomir, G.W. Baxter, S.F. Collins, Effects of High-Temperature Heat Treatment On Nd^{3+}-Doped Optical Fibers for use in Fluorescence Intensity Ratio Based Temperature Sensing, Rev Sci Instrum, 74(2003) 3524-30, https://doi.org/10.1063/1.1578706.

[59] S.F. Collins, G.W. Baxter, S.A. Wade, P.M. Farrell, Strain Dependence of Fluorescence from Rare-Earth-Doped Optical Fibres: Application to the Simultaneous, Co-Located, Measurement of Strain and Temperature, Compos Struct, 58(2002) 373-9, https://doi.org/10.1016/S0263-8223(02)00198-8.